Available online at www.sciencedirect.com
SCIENCE DIRECT®
International Journal of Solids and Structures 42 (2005) 4758–4778
INTERNATIONAL JOURNAL OF SOLIDS and STRUCTURES
www.elsevier.com/locate/ijsolstr

Thermo-mechanical behaviour of rubber materials during vulcanization

M. André [a], P. Wriggers [b,*]

[a] Development of Mechanics and Simulation, Continental AG, Hannover, Germany
[b] Institute for Mechanics and Computational Mechanics, University of Hannover, Appelstr. 9a, 30167 Hannover, Germany

Received 6 May 2004; received in revised form 18 January 2005
Available online 26 February 2005

Abstract

This work focusses on the description of the reaction kinetics and thermomechanical effects during the vulcanization process of rubber materials. Based on the concept of internal variables a model for predicting the local state of vulcanization depending on the temperature history is introduced. Furthermore, a continuum-mechanical material model is presented that includes viscous and inelastic effects. The model is able to cover the material behaviour in the uncured and in the cured state and includes the dependance on temperature. From a set of experiments the parameters of this constitutive model are determined for a selected rubber material on the basis of a genetic algorithm.

Keywords: Material modelling; Thermo-mechanical coupling; Rubber; Vulcanization; Parameter identification

1. Introduction

The numerical simulation of production processes plays an important role in the improvement of product quality, in reducing the product development time and in generating a deeper understanding of industrial processes. Although the performance of hardware and software used in industrial simulation tasks has increased continuously during the last years, there is still a huge need for suitable material models and for reliable procedures to determine material parameters for refined constitutive models. In process simulation, like the production of rubber sealings that is considered in this work, usually coupled field equations have to be solved and often the material behaviour cannot be considered to be constant during the process. This

* Corresponding author. Tel.: +49 5117622220; fax: +49 5117625496.
E-mail address: wriggers@ibnm.uni-hannover.de (P. Wriggers).

0020-7683/$ - see front matter © 2005 Elsevier Ltd. All rights reserved.
doi:10.1016/j.ijsolstr.2005.01.015

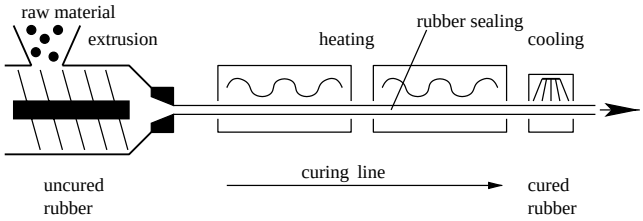

Fig. 1. Extrusion and curing process of rubber sealings.

requires the introduction of complex material models that include inelastic effects with a strongly rate-dependent behaviour and the dependency on additional variables like temperature, state of chemical reactions, etc.

In this work we will develop a constitutive framework for the computational prediction of the production process of rubber sealings including the associated parameter identification procedure from a minimum number of experimental tests. Please refer to Fig. 1 for an overview of the production process. The process starts with the still uncured material that has just left the die of the extruder. Then due to the applied heating, the vulcanization process is initiated. This also yields a deformation of the rubber structure in the heating lines due to gravity forces. The constitutive model should be applicable to predict the final shape of the rubber sealing. Since the state of vulcanization (curing) can be predicted during the heating process, adjustment of the heating parameters is possible in order to optimize the curing process and the tolerances of the final shape of the rubber sealings. During the vulcanization process chemical and electrochemical reactions can occur. However, this paper is focused on chemical reactions only.

For this purpose a chemical reaction model is developed in Section 2 that describes the vulcanization process on the basis of internal variables Coleman (1964) and Coleman and Gurtin (1967). These variables can be used within a continuum mechanical frame and, thus, allow to model the vulcanization within a computational analysis. Afterwards, in Section 3 a suitable material model is introduced that shows visco-elastic effects, plastic effects and that includes the dependence on temperature and the state of the vulcanization process. Experiments that are needed to determine the set of material parameters of this model are described in Section 4. Experimental results are shown and used for an exemplary identification of material parameters.

2. Chemical reactions

Rubber material mainly consists of a large amount of long polymer chains, stochastically distributed and orientated in space. In the uncured state, shown in Fig. 2a, these chains are not connected by cross-links between each other and movement between them is possible. On a macroscopic basis this can be observed

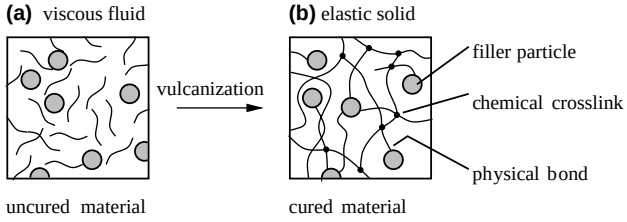

Fig. 2. Molecular model of vulcanization process.

as inelastic (plastic) behaviour that is intentionally used during the molding process of rubber products. Nevertheless, physical links and entanglements between the molecules and links between rubber and filler particles cause some viscous and elastic effects. Therefore, it is reasonable to describe such materials as a viscous fluid. After vulcanization, in the cured state, additional chemical cross-links between the chains prevent them from extended relative movement and, thus, the ability to undergo plastic deformation vanishes, see Fig. 2b for an illustration. A completely cured rubber material will instead show a clear elastic behaviour that can be explained by molecular network models, e.g. Treloar (1975) and Mark (1994). When considering (carbon black) filled rubber compounds a strong viscous behaviour is superposed to the purely elastic response, what can be explained by reorganization effects between the rubber molecules and the filler particles.

A result of this molecular model is that homogenized mechanical properties will strongly depend on the state of vulcanization. With the change from an uncured to a cured material, going along with an increasing density of cross-links, the mechanical behaviour will change from a more fluid-like (plastic) behaviour to a mostly solid-like (elastic) behaviour. Thus, in order to achieve an accurate constitutive model for the coupled thermo-mechanical process, the chemical vulcanization needs to be described sufficiently.

The industrial vulcanization process usually consists of several reactions, in which many different phases interact. A model which includes all these reactions is usually too complex. Here, a simplified two-step vulcanization model that is represented by two chemical reactions is proposed. The first step is a preliminary reaction, described by

$$m_A A + m_B B \rightarrow C. \tag{1}$$

In this first reaction the components A and B react and produce the new phase C. While component B can be interpreted as the raw, totally uncured rubber molecules, the component A represents some vulcanization agent. Then phase C represents any component that is required for further reaction to the finally cross-linked material E. This cross-linking reaction, in which a phase E is produced from components C and D, is described by

$$m_C C + m_D D \rightarrow E. \tag{2}$$

Here, the stochiometric ratio of the reactions is given by the rational numbers m_A, m_B and m_C, m_D, respectively. Furthermore, the concentration of a phase X is expressed by $[X]$ in parts per volume. For the preliminary reaction (1) we obtain the relation

$$[\dot{C}]^{(1)} = -\frac{1}{m_A}[\dot{A}] = -\frac{1}{m_B}[\dot{B}] \tag{3}$$

for the reaction rate $[\dot{C}] = \partial[C]/\partial t$ from the conservation of mass. The reaction rates for the second reaction (2) are

$$[\dot{E}] = -\frac{1}{m_C}[\dot{C}]^{(2)} = -\frac{1}{m_D}[\dot{D}]. \tag{4}$$

Note, that the total reaction rate $[\dot{C}]$ of component C is determined by both reactions and, thus,

$$[\dot{C}] = [\dot{C}]^{(1)} + [\dot{C}]^{(2)}. \tag{5}$$

The velocity of a reaction is usually given by a kinetic approach (see e.g. Atkins, 1982; Laidler, 1963; Schmidt, 1998) of the type

$$[\dot{C}]^{(1)} \sim [A]^{\alpha}[B]^{\gamma}, \tag{6}$$

$$[\dot{E}] \sim [C]^{\beta}[D]^{\delta}. \tag{7}$$

with the orders of the reactions α, γ, β and δ, respectively. When assuming that the cross-linking agent A has a much lower concentration than the component B, the concentration $[B]$ will not change significantly during the reaction and the approximation

$$[B] \approx [B]_0 \approx [B]_\infty \tag{8}$$

can be made. Hereby, the kinetic approach can be simplified to

$$[\dot{C}]^{(1)} \sim [A]^\alpha \tag{9}$$

for the preliminary reaction (1). Following the same considerations the kinetic approach for the second reaction step (2) is simplified

$$[\dot{E}] \sim [C]^\beta. \tag{10}$$

Since the introduced two-step vulcanization model is a simplified approach for a quite complex reaction, the kinetic approaches (9) and (10) are empiric but can be justified by the successful comparison to experimental results that are presented later. The initial conditions for the concentrations before the reaction is started are

$$[A]_0 > 0, \quad [C]_0 = 0, \quad [E]_0 = 0. \tag{11}$$

If, furthermore, the component A is assumed to be used completely during the reaction, its final concentration after completion of the reaction ($t \to \infty$) is

$$[A]_\infty = 0 \tag{12}$$

and this yields the relations

$$[C]_\infty = \frac{1}{m_A}[A]_0, \tag{13}$$

$$[E]_\infty = \frac{1}{m_C}[C]_\infty, \tag{14}$$

$$[A] = [A]_0 - m_A[C] - m_C m_A[E]. \tag{15}$$

By inserting the relationships (15), (9) and (4) into Eq. (5) one obtains

$$[\dot{C}] \sim ([A]_0 - m_A[C] - m_A m_C[E])^\alpha - m_C[\dot{E}]. \tag{16}$$

A material model based on continuum mechanics does not necessarily require the absolute number of cross-links, but is rather described by some internal variables describing the state of the vulcanization process. Therefore, the normalized concentrations

$$\eta = \frac{[C]}{[C]_\infty} \quad \text{and} \quad \zeta = \frac{[E]}{[E]_\infty}, \quad 0 \leqslant \eta, \zeta \leqslant 1 \tag{17}$$

are introduced as internal variables, see e.g. Coleman (1964), Coleman and Gurtin (1967) and Haupt and Olt (1989). Inserting the Eqs. (13) and (14) into Eq. (16) and replacing the concentrations $[C]$ and $[E]$ according to Eq. (17) yields the evolution law for η

$$\dot{\eta} = a(\Theta)(1 - \eta - \zeta)^\alpha - \dot{\zeta}. \tag{18}$$

Applying the same relations to Eq. (10) yields the evolution law for ζ

$$\dot{\zeta} = b(\Theta)\eta^\beta. \tag{19}$$

Finally, the substitution $\xi = \eta + \zeta$ simplifies the Eqs. (18) and (19) to

$$\dot{\xi} = a(\Theta)(1-\xi)^{\alpha}, \tag{20}$$

$$\dot{\zeta} = b(\Theta)(\xi-\zeta)^{\beta}. \tag{21}$$

In this approach the coefficients $a(\Theta)$ and $b(\Theta)$ represent the temperature dependence of the reaction which are assumed to obey the Arrhenius law

$$a(\Theta) = k_1 \exp\left(-\frac{k_2}{\Theta}\right), \tag{22}$$

$$b(\Theta) = k_3 \exp\left(-\frac{k_4}{\Theta}\right) \tag{23}$$

with $k_2 = \frac{E_A}{R}$, $k_4 = \frac{E_B}{R}$.

Here, R is the universal gas constant and E_A and E_B are the activation energies of the corresponding reactions. If the temperature $\Theta(t)$ is given, integration of Eqs. (20) and (21) finally yields the degree of cross-linking $\zeta(t)$, i.e. the state of the vulcanization process. In order to guarantee a monotonously increasing function for $\xi(t)$ and $\zeta(t)$ and an asymptotic approach according to

$$\dot{\xi}(t) \geqslant 0, \quad \xi(t\to\infty) = 1 \quad \text{and} \quad \dot{\zeta}(t) \geqslant 0, \quad \zeta(t\to\infty) = 1 \tag{24}$$

the following restrictions to the coefficients $a(\Theta)$, $b(\Theta)$ and the exponents α, β have to be considered:

$$a(\Theta) \geqslant 0, \quad b(\Theta) \geqslant 0, \quad \alpha > 0, \quad \beta > 0. \tag{25}$$

Since the reaction schemes (1) and (2) only describe a simplified vulcanization model, it is not possible to determine the parameters k_1, k_2, k_3, k_4, α and β from fundamental chemical or physical material data. These parameters need to be determined from experiments for each rubber compound by a parameter identification as described in Section 4. The typical evolution of the state variables $\xi(t)$ and $\zeta(t)$ during an isothermal curing process at $\Theta = 160$ °C using the parameters listed in Section 4 is visualized in Fig. 3. The preliminary reaction is clearly causing a delay at the beginning of the cross-linking reaction.

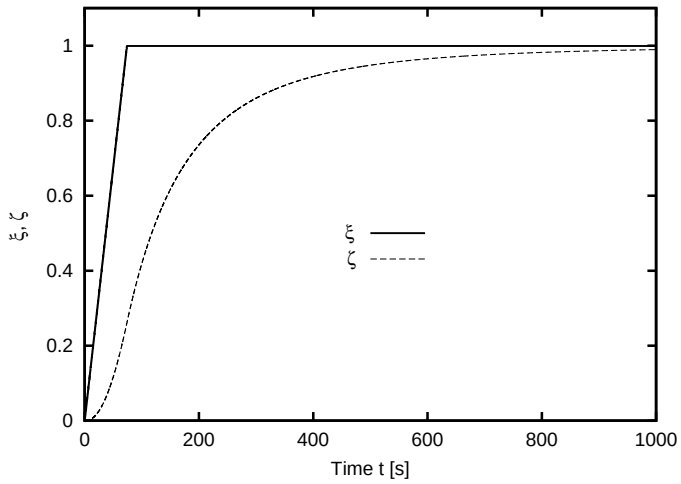

Fig. 3. Evolution of the state variables ξ and ζ at isothermal conditions.

3. Material model

The well known nonlinear stress-strain relationship of rubber materials in the large strain range is usually adequately described by a hyperelastic material model expressed in terms of a strain energy potential. This approach is sufficient when restricting to static and quasi-static problems and when looking at unfilled rubber compounds only. Some popular examples for such strain energy functions are the Neo-Hooke, the Mooney–Rivlin, the Arruda–Boyce, the Yeoh or the Ogden material model. All of these have been discussed extensively in literature and are state-of-the-art in computational solid mechanics, see e.g. Mooney (1940), Ogden (1972) and Ogden (1984).

Nevertheless, when looking at experimental results of dynamically loaded carbon black filled rubber compounds one will clearly realize that a purely elastic approach does not satisfy the need for realistic results. The complex mechanical behaviour of filled rubber materials is also characterized by a strong dependency on temperature, strain rates and load history, even in the small strain range. This fact clearly requires the extension of the common and well-known purely elastic material models for rubber by additional visco-elastic effects. Since this paper deals with the description of rubber during the vulcanization process and the material in the uncured state is characterized by a fluid-like behaviour that makes forming and processing possible, also plastic effects which are causing residual strains need to be covered in an appropriate material model.

Although, rubber is commonly used within applications that might cause extremely high strains and, thus, require the introduction of nonlinear elastic material models in combination with finite deformation kinematics, in this work we assume all strains to be sufficiently small which allows the use of linearized small-strain kinematics. This is reasonable for the investigated production process, because during the heating and curing process of such rubber products large strains do not occur and actually would mean that the final product is unusable. Nevertheless, an extension to a finite kinematics formulation would increase the range of application for the material model proposed here and is subject of future work.

A material model that is fulfilling the above mentioned requirements is introduced in this work and, later on, the physically relevant effects are identified by appropriate experimental results. Since the goal is to describe the material behaviour during processing it is necessary to include dependencies on temperature and state of curing into the material model and also into the testing procedure of the rubber compound for parameter identification.

3.1. Rheological approach

The classic method to describe inelastic behaviour of either elastic, viscous or plastic material is the combination of rheologic elements, each of them defining certain effects. Elastic properties are visualized by spring elements, viscous properties by dashpots and plastic effects by frictional elements. A combination of several of these elements can yield quite complex material behaviour, see e.g. Aklonis and MacKnight (1983), Ferry (1980), Kaliske and Rothert (1997) and Kaliske and Rothert (1998). Connecting two elements in parallel means that the stress contributions from each element are added to a total stress. Connecting them in a line means that the total strain can be split into parts for each rheologic element. Although the visualization of these models is usually associated with uniaxial deformation, the models can be generalized to describe three-dimensional behaviour.

The rheologic elements used in this work are defined in Fig. 4, showing an elastic spring element (a), a Kelvin–Voigt element (b) representing the visco-elastic effects and a Bingham element (c) representing the visco-plastic effects. In addition a symbol (d) is introduced that represents a strain contribution resulting from internal state variables, e.g. the temperature or the state of curing or the evolution of the inelastic material history. A proper combination of these elements allows the description of material behaviour during the vulcanization process including all significant effects of the rubber material in the uncured as well as in the cured state. The relevant model is introduced and visualized in Fig. 5.

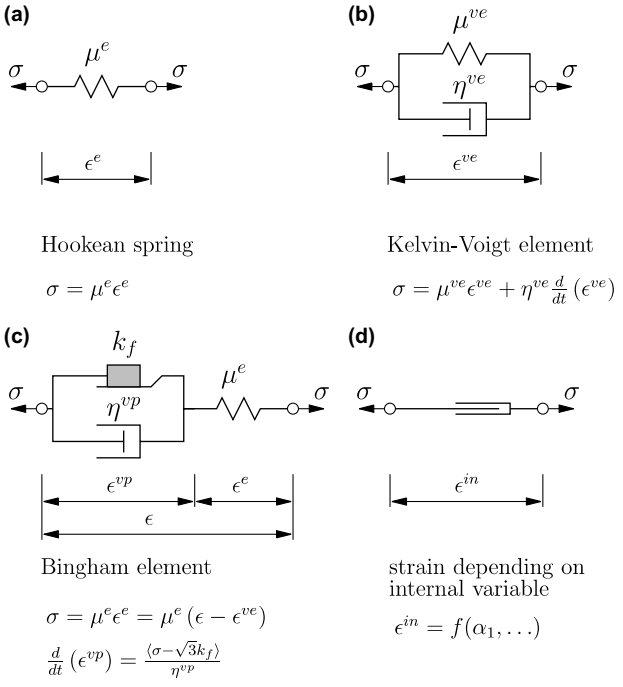

Fig. 4. Rheologic models and their constitutive equations.

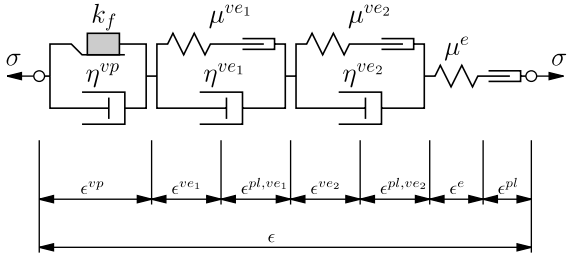

Fig. 5. Additive split of strains into elastic, visco-elastic and visco-plastic parts.

The total strain $\boldsymbol{\epsilon}$ of this model can be split into several parts

$$\boldsymbol{\epsilon} = \boldsymbol{\epsilon}^{\mathrm{e}} + \boldsymbol{\epsilon}^{\mathrm{th}} + \boldsymbol{\epsilon}^{\mathrm{vp}} + \boldsymbol{\epsilon}^{\mathrm{ve_1}} + \boldsymbol{\epsilon}^{\mathrm{ve_2}} + \underbrace{\boldsymbol{\epsilon}^{\mathrm{pl,e}} + \boldsymbol{\epsilon}^{\mathrm{pl,ve_1}} + \boldsymbol{\epsilon}^{\mathrm{pl,ve_2}}}_{\boldsymbol{\epsilon}^{\mathrm{pl}}} \tag{26}$$

with elastic (e), thermal (th), viscoplastic (vp), two viscoelastic ($\mathrm{ve_1}$ and $\mathrm{ve_2}$) and pseudo-plastic (pl) contributions. The necessity to introduce these different parts and their computation is described in detail below. A simulation of the continuous vulcanization process will require the modification of the related material parameters depending on internal variables, i.e. the state of curing ζ and the temperature Θ. Nevertheless, for simplicity reasons these dependencies will not be considered in the following sections that are presenting the rheologic effects and the corresponding material models. The dependencies will instead be introduced afterwards in Section 3.6.

3.2. Elastic material behaviour

When applying a certain load to a rubber sample this results in an instantaneous deformation. If this deformation vanishes immediately and completely after unloading the sample, this is a purely elastic behaviour. Although rubber usually requires a more advanced modelling, e.g. by using a hyperelastic strain energy function, we will use the linear elastic Hooke's law. This implies the restriction to small strains, what has already been mentioned and justified to be sufficient.

The elastic strain tensor $\boldsymbol{\epsilon}^{\mathrm{e}}$ can be split into a volume changing part

$$e_v^{\mathrm{e}}\mathbf{1} = \frac{1}{3}\mathrm{tr}(\boldsymbol{\epsilon}^{\mathrm{e}})\mathbf{1} \tag{27}$$

and a deviatoric, isochoric part

$$\boldsymbol{e}^{\mathrm{e}} = \boldsymbol{\epsilon}^{\mathrm{e}} - e_v^{\mathrm{e}}\mathbf{1}. \tag{28}$$

The linear-elastic material law then is defined by

$$\boldsymbol{\sigma} = p^{\mathrm{e}}\mathbf{1} + \boldsymbol{s}^{\mathrm{e}} = K^{\mathrm{e}}e_v^{\mathrm{e}}\mathbf{1} + 2\mu^{\mathrm{e}}\boldsymbol{e}^{\mathrm{e}} \tag{29}$$

with K^{e} denoting the elastic bulk modulus, μ^{e} the elastic shear modulus. Here the stress tensor $\boldsymbol{\sigma}$ has also been split into a pressure part $p^{\mathrm{e}}\mathbf{1}$ and into a stress deviator $\boldsymbol{s}^{\mathrm{e}}$. It has to be mentioned that rubber material is observed to be nearly incompressible, what results in a relatively high bulk modulus K^{e} and needs some special attention in a numerical treatment.

Thermal expansion or shrinkage is defined by the thermal strain tensor

$$\boldsymbol{\epsilon}^{\mathrm{th}} = \alpha^{\mathrm{th}}\Delta\Theta\mathbf{1}, \tag{30}$$

with $\Delta\Theta$ denoting the difference between the material temperature and a reference temperature in which the material is assumed to be free of thermal strains. The thermal expansion coefficient is α^{th}.

3.3. Visco-elastic material behaviour

In addition to a purely elastic and a thermal strain component the introduced material model includes two visco-elastic components described by Kelvin–Voigt elements, each representing a linear visco-elastic behaviour with characteristic relaxation times τ_1^{ve} and τ_2^{ve}, respectively. Since rubber material is well described by an almost incompressible behaviour the assumption of a purely deviatoric visco-elastic deformation is reasonable. Thus, the visco-elastic strain rates for each Kelvin–Voigt element are driven by the stress deviator $\boldsymbol{s}^{\mathrm{e}} = 2\mu^{\mathrm{e}}\boldsymbol{e}^{\mathrm{e}}$ and are determined by the evolution laws

$$\dot{\boldsymbol{e}}^{\mathrm{ve}_1} = \frac{1}{\eta^{\mathrm{ve}_1}}(\boldsymbol{s}^{\mathrm{e}} - 2\mu^{\mathrm{ve}_1}\boldsymbol{e}^{\mathrm{ve}_1}), \tag{31}$$

$$\dot{\boldsymbol{e}}^{\mathrm{ve}_2} = \frac{1}{\eta^{\mathrm{ve}_2}}(\boldsymbol{s}^{\mathrm{e}} - 2\mu^{\mathrm{ve}_2}\boldsymbol{e}^{\mathrm{ve}_2}). \tag{32}$$

These equations can be simplified which yields

$$\dot{\boldsymbol{e}}^{\mathrm{ve}_1} = B_1\boldsymbol{e}^{\mathrm{e}} - B_2\boldsymbol{e}^{\mathrm{ve}_1}, \tag{33}$$

$$\dot{\boldsymbol{e}}^{\mathrm{ve}_2} = B_3\boldsymbol{e}^{\mathrm{e}} - B_4\boldsymbol{e}^{\mathrm{ve}_2} \tag{34}$$

with the abbreviations

$$B_1 = 2\frac{\mu^{\mathrm{e}}}{\eta^{\mathrm{ve}_1}}, \quad B_2 = 2\frac{\mu^{\mathrm{ve}_1}}{\eta^{\mathrm{ve}_1}}, \quad B_3 = 2\frac{\mu^{\mathrm{e}}}{\eta^{\mathrm{ve}_2}}, \quad B_4 = 2\frac{\mu^{\mathrm{ve}_2}}{\eta^{\mathrm{ve}_2}}. \tag{35}$$

Note, that it is necessary to extend these evolution equations by so-called pseudoplastic contributions if the material parameters μ^{e}, μ^{ve_1} and μ^{ve_2} are changing during the process, see Section 3.5 and Section 3.6 for details. This is obvious happening in the case of the vulcanization process.

3.4. Visco-plastic response

In addition to the already introduced instantaneous elastic and rate dependent visco-elastic properties, rubber material also depicts plastic behaviour under certain conditions. From a molecular point of view, plastic effects usually occur if polymer chains that have been stretched are able to reorganize within the polymer structure and, thus, can generate a new state with reduced mechanical stresses. This is possible when no or only few cross-links exist and is of importance especially in the uncured state. Plastic deformation is intentionally used in the molding process in order to give the product the desired shape. Since the reorganization of the polymers is a time dependent process, plasticity will be described in this work by a visco-plastic flow rule. During the curing process the increasing number of cross-links will more and more reduce the ability of polymer chains to reorganize. Finally, plastic flow is completely stopped and the material can be considered to be elastic in the cured state.

In this work a von-Mises yield criterion based on the second invariant of the stress deviator defines the elastic state, see e.g. Simo and Hughes (1998)

$$\Phi(\boldsymbol{s}^{e}) = \sqrt{J_2} - k_{\mathrm{f}} \leqslant 0 \tag{36}$$

$$\text{with} \quad J_2 = \frac{1}{2}\boldsymbol{s}^{\mathrm{e}} : \boldsymbol{s}^{\mathrm{e}}. \tag{37}$$

Here, the parameter k_{f} is the yield limit determined by a pure shear test. Since the material's ability to undergo plastic deformation is restricted to nearly uncured rubber the yield limit k_{f} depends on the degree of cross-linking ζ. For high degress of cross-linking above the gel point the yield limit k_{f} must reach very high values in order to prevent plastic flow completely.

In the case of yielding, i.e. if $\Phi(\boldsymbol{s}^{e}) > 0$, the visco-plastic flow rate $\dot{\boldsymbol{e}}^{\mathrm{vp}}$ is defined by the associated flow rule

$$\dot{\boldsymbol{e}}^{\mathrm{vp}} = \lambda^{\mathrm{vp}}\boldsymbol{s}^{\mathrm{e}}. \tag{38}$$

The parameter λ^{vp} is determined from

$$\lambda^{\mathrm{vp}} = \begin{cases} 0 & \text{if } \sqrt{J_2} \leqslant k_{\mathrm{f}}, \\ \frac{1}{2\eta^{\mathrm{vp}}}\left(1 - \frac{k_{\mathrm{f}}}{\sqrt{J_2}}\right) & \text{if } \sqrt{J_2} > k_{\mathrm{f}}. \end{cases} \tag{39}$$

3.5. Pseudo-plastic strains

Unless the model is extended by some additional effects the application of the constitutive model introduced above for the analysis of the curing process can yield unreasonable results. This is due to the fact that the constitutive model will require that some material parameters, e.g. the elastic shear modulus μ^{e}, are depending on the degree of cross-linking ζ. For a consistent constitutive model which is in accordance with thermodynamical restrictions it is necessary to introduce additional inelastic strain components which are changing the stress-free state of the material. The necessity to introduce these strains, in this context called pseudo-plastic strains, becomes obvious when looking at the situation depicted in Fig. 6.

Here we consider an only slightly cross-linked rubber sample ($\zeta_0 \ll 1$) like shown in Fig. 6a which is assumed to be free of stresses and strains in the initial state. For simplicity, visco-elastic and plastic effects will be neglected in this simple experiment. Therefore, the instantaneous stress response after uniaxial loading of

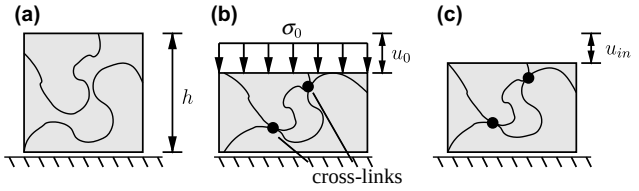

Fig. 6. Residual strains due to cross-linking.

the sample (Fig. 6b) is assumed to be linear elastic according to Eq. (29). Under the condition of incompressibility the stress in loading direction is simply given by

$$\sigma_0 = E_0^{\mathrm{e}} \frac{u_0}{h} = 3\mu_0^{\mathrm{e}}\, \epsilon_0^{\mathrm{e}}. \tag{40}$$

Since material properties are changing during the process of cross-linking, the elastic shear modulus μ^{e} will be a function of temperature Θ and of the state of cross-linking ζ

$$\mu^{\mathrm{e}} = f_\mu(\Theta, \zeta). \tag{41}$$

During vulcanization an increasing number of cross-links ($\zeta_1 > \zeta_0$) at assumed isothermal conditions ($\Theta = \Theta_0 = \Theta_1$) will clearly yield an increase in the elastic shear modulus Treloar (1975)

$$\mu_1^{\mathrm{e}} = f_\mu(\Theta, \zeta_1) > \mu_0^{\mathrm{e}} = f_\mu(\Theta, \zeta_0). \tag{42}$$

This increase in the shear modulus would cause an increase in the stress response

$$\sigma_1 = 3\mu_1^{\mathrm{e}}\, \epsilon^{\mathrm{e}} > \sigma_0 = 3\mu_0^{\mathrm{e}}\, \epsilon^{\mathrm{e}}, \tag{43}$$

even when no further deformation is applied ($\epsilon^{\mathrm{e}} = \epsilon_1^{\mathrm{e}} = \epsilon_0^{\mathrm{e}}$). This is clearly not reasonable, since the increased stored strain energy would violate thermodynamic principles. In Adolf et al. (1998) a visco-elastic approach in conjunction with a convolution integral is used to overcome this problem.

The mentioned effect can also be avoided by introducing additional inelastic strains ϵ^{in}. Assuming linearized kinematics, the total strain is additively split into an elastic part that determines the elastic stresses and an inelastic part that needs to be determined in agreement with the above considerations

$$\epsilon = \epsilon^{\mathrm{e}} + \epsilon^{\mathrm{in}}. \tag{44}$$

A reasonable assumption is that a change in the state of curing ζ, may change the material's shear modulus μ^{e}, but must not change the stress response σ. This yields the requirement

$$\frac{\partial \sigma}{\partial \zeta} = 0. \tag{45}$$

In this paper the stress σ is assumed to depend linearly on the elastic part of the strain ϵ^{e} according to Eq. (40)

$$\sigma = 3\mu^{\mathrm{e}}\epsilon^{\mathrm{e}}. \tag{46}$$

Then Eq. (45) can be written as

$$\frac{\partial \sigma}{\partial \zeta} = 3\left(\frac{\partial \mu^{\mathrm{e}}}{\partial \zeta}\epsilon^{\mathrm{e}} + \mu^{\mathrm{e}}\frac{\partial \epsilon^{\mathrm{e}}}{\partial \zeta}\right) = 0. \tag{47}$$

Since the total strain ϵ does not depend on the state of cross-linking ζ, applying Eq. (44) to the second term in the brackets of Eq. (47) yields

$$\frac{\partial \mu^{e}}{\partial \zeta}\epsilon^{e} + \mu^{e}\underbrace{\frac{\partial \epsilon}{\partial \zeta}}_{=0} - \mu^{e}\frac{\partial \epsilon^{in}}{\partial \zeta} = 0 \tag{48}$$

and an evolution law for the inelastic strains ϵ^{in} can be derived

$$\frac{\partial \epsilon^{in}}{\partial \zeta} = \frac{\partial \mu}{\partial \zeta}\frac{\epsilon^{e}}{\mu^{e}}. \tag{49}$$

This evolution law can easily be generalized to a spatial description and the evolution law for the pseudo-plastic strain tensor is

$$\dot{\boldsymbol{\epsilon}}^{in,e} = B_7\boldsymbol{\epsilon}^{e} \tag{50}$$

with the abbreviation

$$B_7 = \frac{\partial \mu^{e}}{\partial \zeta}\frac{\dot{\zeta}}{\mu^{e}}. \tag{51}$$

The visco-elastic parts of the introduced material model need to be extended by pseudo-plastic strain parts, following just the same arguments and derivations. Thus, Eqs. (33) and (34) have to be replaced by

$$\dot{\boldsymbol{e}}^{ve_1} = B_1\boldsymbol{e}^{e} - B_2\boldsymbol{e}^{ve_1} - \dot{\boldsymbol{e}}^{in,ve_1}, \tag{52}$$

$$\dot{\boldsymbol{e}}^{ve_2} = B_3\boldsymbol{e}^{e} - B_4\boldsymbol{e}^{ve_2} - \dot{\boldsymbol{e}}^{in,ve_2}. \tag{53}$$

The corresponding evolution laws are

$$\dot{\boldsymbol{e}}^{in,ve_1} = B_5\boldsymbol{e}^{ve_1}, \tag{54}$$

$$\dot{\boldsymbol{e}}^{in,ve_2} = B_6\boldsymbol{e}^{ve_2} \tag{55}$$

with the abbreviations

$$B_5 = \frac{\partial \mu^{ve_1}}{\partial \zeta}\frac{\dot{\zeta}}{\mu^{ve_1}}, \quad B_6 = \frac{\partial \mu^{ve_2}}{\partial \zeta}\frac{\dot{\zeta}}{\mu^{ve_2}} \tag{56}$$

and finally all pseudo-plastic strain parts can be summarized as

$$\dot{\boldsymbol{\epsilon}}^{in} = \dot{\boldsymbol{e}}^{in,ve_1} + \dot{\boldsymbol{e}}^{in,ve_2} + \dot{\boldsymbol{\epsilon}}^{in,e}. \tag{57}$$

3.6. Dependence on temperature and state of cross-linking

The introduced material model contains the parameters

$$\mu^{e},\ \mu^{ve_1},\ \mu^{ve_2},\ \eta^{ve_1},\ \eta^{ve_2},\ \eta^{vp}, k_f. \tag{58}$$

So far, all constitutive equations and their parameters have been considered for isothermal conditions ($\Theta = \text{const.}$) and at a constant state of cross-linking ($\zeta = \text{const.}$). A realistic description of the vulcanization process needs to consider the dependence of the mechanical properties on temperature and state of cross-linking.

The following functions describing these dependencies are defined on an empirical basis which is backed up by experiments, see Section 4.

The elastic parameters in terms of the shear moduli show the following dependence on the temperature Θ and the state of vulcanization ζ

$$\mu^{e} = (p_1 + p_2\zeta) f_1(\Theta), \tag{59}$$

$$\mu^{ve_1} = p_{10}\mu^{e}, \tag{60}$$

$$\mu^{ve_2} = (p_3 + p_4\zeta)\mu^{e}, \tag{61}$$

with

$$f_1(\Theta) = (p_8 - \Theta)^{p_9}. \tag{62}$$

The viscous parameters obey the relations

$$\eta^{ve_1} = p_{11} f_1(\Theta), \tag{63}$$

$$\eta^{ve_2} = p_5 \mu^{ve_2}, \tag{64}$$

$$\eta^{vp} = p_{12}\mu^{e} \tag{65}$$

and the relaxation times of the visco-elastic elements are given by

$$\tau^{ve_1} = \frac{\eta^{ve_1}}{\mu^{ve_1}} = \frac{p_{11}}{p_{10}(p_1 + p_2\zeta)}, \tag{66}$$

$$\tau^{ve_2} = \frac{\eta^{ve_2}}{\mu^{ve_2}} = p_5. \tag{67}$$

Finally, the yield value of the visco-plastic element is defined by

$$k_f = -p_6 \log(1 - \zeta) f_2(\Theta), \tag{68}$$

with

$$f_2(\Theta) = \frac{\Theta_0}{\Theta - p_7} \tag{69}$$

which depends on temperature and vulcanization state.

In order to guarantee positive elastic moduli and thermodynamical reasonable results, all constants p_i are assumed to be positive

$$p_i > 0, \quad i = 1, \ldots, 12 \tag{70}$$

and the following restriction applies to the constants p_7 and p_8

$$p_7 < \Theta < p_8. \tag{71}$$

All constants p_i need to be identified by suitable experimental results that cover the relevant temperature range and material effects in the uncured as well as in the cured state.

4. Experimental results and parameter identification

In this section we describe the experiments that are needed to determine all constitutive parameters introduced so far for the chemo-thermo-mechanical material equations. Due to the complexity of the experiments involving the curing process in dependency on temperature and mechanical state we targeted to use only a minimal number of different experimental setups. This is the vulkameter test equipment, see e.g. Haupt and Olt (1989), which is commonly applied in rubber industry and a special uniaxial compression test. With these two experimental setups it is possible to determine all constitutive parameters by

running an appropriate set of tests at different temperatures and curing states. An EPDM rubber compound has been used in order to demonstrate the experiments and the procedure of parameter identification.

4.1. Procedure of parameter identification

The goal of a parameter identification is to choose the free parameters of a given constitutive model in such a way that the response of the model is representing the real material as good as possible. For some simple material models with very few parameters this can often be done by a manual evaluation of the experimental data. But if the material model is more complex and, thus, the number of parameters that have to be determined from experiments increases, an automated procedure is necessary. An easy-to-use and comfortable method for such purposes are genetic algorithms. The basic idea and the use of the genetic algorithm that has been used in this work is explained in this section. For an overview also see references Davis (1991) and Yeo and Agyei (1998).

The complete experimental data that will be used for the parameter identification is arranged in n_f sets of data, where each set represents one test. One set k ($k = 1, \ldots, n_f$) contains the load function $G^k(t)$ that is applied to the specimen (e.g. a displacement function) and the measured response $F^k(t)$ (e.g. a reaction force). Additional boundary and testing conditions with influence on the material response, e.g. temperature, are summarized in a vector $\boldsymbol{p}^k = (p_1^k, p_2^k, \ldots)$ for each test k. These parameters can be used in the evaluation of the constitutive equation, but are no free parameters that need to be determined. Since a computational treatment usually requires discrete values the continuous load functions $G^k(t)$ and the response function $F^k(t)$ will be stored as a series of $m+1$ discrete values $\widetilde{G}^k(t_i)$ and $\widetilde{F}^k(t_i)$ at times t_i, $i = 0, \ldots, m$ as visualized in Fig. 7.

For further treatment the free parameters of the constitutive model are arranged in a solution vector

$$\boldsymbol{q} = q_j, \; j = 1, \ldots, n_q \tag{72}$$

with n_q components. A lower and upper bound

$$q_j^{\min} \leqslant q_j \leqslant q_j^{\max} \tag{73}$$

is defined for each parameter in order to limit the valid range and define an interval for the search algorithm. Assuming the material parameters $\boldsymbol{q}$ to be known, the response function $f^k(t, \boldsymbol{q}, \boldsymbol{p}, G^k)$ can be determined for a certain set of parameters $\boldsymbol{q}$ at a given load G^k and additional testing parameters $\boldsymbol{p}^k$. The response function is stored as a series of discrete values $\tilde{f}^k(t_i, \boldsymbol{q}, \boldsymbol{p}^k, \widetilde{G}^k)$ at times t_i for each test k. Since the constitutive model used in this work contains history dependent internal variables (e.g. the state of

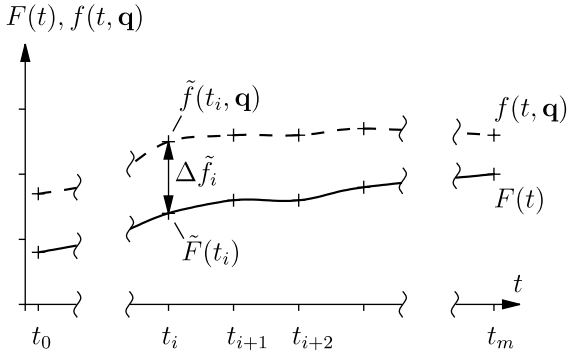

Fig. 7. Deviation $\Delta\tilde{f}_i$ between measurement $\widetilde{F}(t_i)$ and simulated response $\tilde{f}(t_i, \boldsymbol{q})$.

vulcanization) the response function is defined by differential equations that need to be solved by integration over time.

The solution of the parameter identification is obtained, if the computed response function f^k and the measured data F^k are the same for all experiments:

$$f^k(t, \boldsymbol{q}, \boldsymbol{p}^k, G^k) = F^k(t) \quad \forall k \in [1, \ldots, n_\mathrm{f}]. \tag{74}$$

An additional requirement is that the set of experiments used is sufficiently covering the physical effects of the material. This yields an inverse problem

$$\boldsymbol{q} = f^{-1}(F, \boldsymbol{p}, G) \tag{75}$$

what is usually an ill-posed problem and cannot be solved directly Mahnken (1993).

Instead, a total deviation $\widetilde{A}(\boldsymbol{q})$ between experimental results and predicted response function is defined and minimized by an appropriate algorithm. The total deviation is defined by

$$\widetilde{A}(\boldsymbol{q}) = \sum_{k=1}^{n_\mathrm{f}} \widetilde{A}^k(\boldsymbol{q}) \tag{76}$$

with the contributions $\widetilde{A}^k$ from each test k defined by

$$\widetilde{A}^k(\boldsymbol{q}) = \sum_{i=0}^{m^k} w_i^k (\Delta \tilde{f}_i^k)^2, \tag{77}$$

$$\Delta \tilde{f}_i^k = \widetilde{F}^k(t_i) - \tilde{f}^k(t_i, \boldsymbol{q}, \boldsymbol{p}^k, \widetilde{G}^k). \tag{78}$$

The weighting factors w_i^k allow the use of time steps $\Delta t_i = t_{i+1} - t_i$ that are not constant by choosing

$$w_0^k = \frac{1}{2}(t_1^k - t_0^k), \tag{79}$$

$$w_i^k = \frac{1}{2}(t_{i+1}^k - t_{i-1}^k), \quad i = 1, \ldots, (m^k - 1), \tag{80}$$

$$w_{m^k}^k = \frac{1}{2}(t_{m^k}^k - t_{m^k-1}^k). \tag{81}$$

The weighting factors can also be used in order to emphasize certain time intervals of the experiment and, thus, achieve a higher accuracy of the identified parameters for certain loading or boundary conditions.

A genetic algorithm is used to determine a parameter set $\boldsymbol{q}$ that minimizes the deviation defined in Eq. (76). First, an initial solution vector $\boldsymbol{q}^0$ needs to be defined. By applying random changes to this vector $\boldsymbol{q}^0$ a first generation $G_\mathrm{C}^1 = (\boldsymbol{q}_1^1, \ldots, \boldsymbol{q}_{n_\mathrm{C}}^1)$ with n_C parameter vectors is generated. For each solution vector $\boldsymbol{q}_y^1$ the deviation $\widetilde{A}(\boldsymbol{q}_y^1)$ is computed and stored. Then the n_P vectors with the lowest deviation are selected from the generation G_C^1, where $n_\mathrm{P} < n_\mathrm{C}$. Only these form the new parent generation $G_\mathrm{P}^1 = (\boldsymbol{q}_1^1, \ldots, \boldsymbol{q}_{n_\mathrm{P}}^1)$ from which a new child generation G_C^2 is produced by random combination and modification of the parameter vectors in G_P^1. The modification has to asure that the limits defined by (73) are not violated. Then the algorithm proceeds with a new selection, defining the next parent generation. This scheme is repeated until the deviation has reached a defined minimum or no further improvement can be achieved. Typical numbers of parent and child vectors used in the genetic algorithm are $n_\mathrm{P} = 500$, $n_\mathrm{C} = 3000$ and between 30 and 60 generations have to be evaluated, before the solution vector $\boldsymbol{q}$ is sufficiently accurate. Such a genetic algorithm provides a very comfortable tool for parameter identification, because it usually does not get trapped by local minima and does not suffer from convergence problems as it might happen to gradient based algorithms.

4.2. Cyclic vulkameter tests

The vulkameter test is a standard experiment that is commonly used for the characterization of rubber properties during processing. The dependence of mechanical properties on the state of vulcanization is investigated in order to measure the progress of the vulcanization process under isothermal conditions. In this work it is also used to determine some elastic and visco-elastic parameters as a function of vulcanization and temperature.

The experimental setup of the vulkameter test is visualized in Fig. 8. An uncured, disc-shaped rubber sample is inserted into the testing chamber of the vulkameter. The sample is heated at a defined temperature Θ_h. Since it is sufficiently small and thin, a constant and homogeneous temperature $\Theta = \Theta_h$ can be assumed after a short time. In addition, a cyclic harmonic torsion angle

$$\varphi(t) = \hat{\varphi}\sin(\omega t) \tag{82}$$

is applied to the rubber sample. This shear deformation yields a torque response $M(t)$ that is measured by the test equipment. The torque $M(t)$ is plotted versus time t which yields the dependency of $M(t)$ on the vulcanization state, see Fig. 9. This information can already be used to determine the vulcanization parameters introduced in Section 2. Details will be discussed in Section 4.2.1.

Furthermore, the simplification of the quite complex material model, introduced in Fig. 5, to a reduced model shown in Fig. 10 allows the determination of some mechanical properties from the vulkameter test. Visco-elastic effects with very large relaxation times can be neglected since the frequency applied to the sample in the vulkameter test is usually $f = \frac{\omega}{2\pi} = 0.8333\ \mathrm{s}^{-1}$ and, thus, only the first Kelvin–Voigt element needs to be considered in this context. The second Kelvin–Voigt element, whose parameters will be determined later, shows typical relaxation times of $\tau^{\mathrm{ve}_2} > 400$ s, so that the assumption made above holds and the torque response can be described by

$$M(t) = \widehat{M}(t)\sin\left(\omega t + \delta(t)\right). \tag{83}$$

Here, $\widehat{M}(t)$ denotes the amplitude of the cyclic torque $M(t)$, ω is the angular frequency of the torsional load and $\delta(t)$ is the phase angle between torsion and torque. Note that also plastic and pseudo-plastic effects do not need to be considered in this experiment, since the integral of such inelastic effects will vanish after completion of one cycle and the variations within one cycle will be sufficiently small.

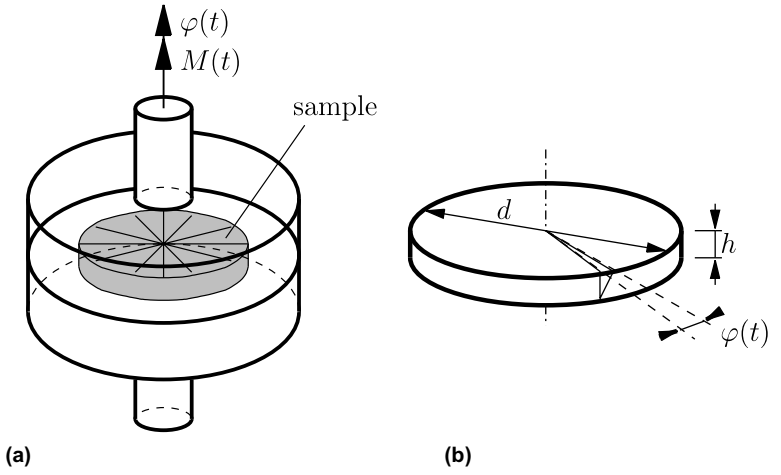

Fig. 8. (a) Vulkameter test equipment and (b) geometry of sample.

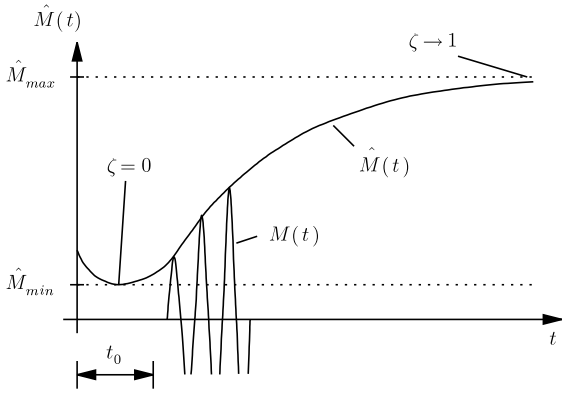

Fig. 9. Torque measurement during vulkameter test.

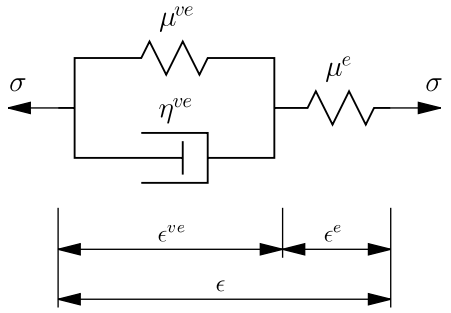

Fig. 10. Simplified rheologic model.

This model allows the analytical determination of the torque value from the material parameters μ^{e}, μ^{ve_1}, η^{ve_1} on the basis of the fundamental St. Venant theory of torsion. This yields the torque response

$$M(t) = \frac{\mu^{e} I_T}{h} \varphi^{e}(t) \tag{84}$$

with the torsional moment of inertia of a disc-shaped structure

$$I_T = \frac{\pi d^4}{32}. \tag{85}$$

Eq. (26) applied to the simplified material model requires a split of the torsional deformation into an elastic part ϕ^{e} and a visco-elastic part ϕ^{ve_1} according to

$$\phi(t) = \phi^{e}(t) + \phi^{ve_1}(t) \tag{86}$$

and the torque then is determined by

$$M(t) = \widehat{M}^{*}(t) \sin(\omega t) + \widehat{M}^{**}(t) \cos(\omega t) \tag{87}$$

with

$$\widehat{M}^{*}(t) = \frac{\mu^{e} I_T}{h} (\hat{\varphi} - C_1)$$

$$\widehat{M}^{**}(t) = -\frac{\mu^{e} I_{T}}{h} C_2.$$

The coefficients C_1 and C_2 are derived from Eq. (35)

$$C_1 = \frac{(B_1 + B_2)B_1\hat{\varphi}}{(B_1 + B_2)^2 - \omega^2}, \quad C_2 = \frac{B_1\hat{\varphi}\ \omega}{(B_1 + B_2)^2 - \omega^2}. \tag{88}$$

Hence the torque response can be split into a part $M^*(t)$ that is in-phase to the torsional deformation $\varphi(t) = \hat{\varphi}\sin(\omega t)$ and an out-of-phase part $M^{**}(t)$. The phase angle $\delta(t)$ is usually expressed in terms of its tangent

$$\tan\delta(t) = \frac{\widehat{M}^{**}(t)}{\widehat{M}^{*}(t)} = -\frac{C_2}{\hat{\varphi} - C_1}. \tag{89}$$

The standard output of the vulkameter test is the amplitude of the torque $\widehat{M}(t)$ and the tangent of the phase angle $\delta(t)$. These values will be used in the following for the identification of material parameters.

4.2.1. Curing parameters

In a first step only the amplitude of the moment $\widehat{M}(t)$ will be used to determine the kinetics of the vulcanization process. According to Eqs. (59) and (62) the elastic shear modulus μ^{e} depends on the state of cross-linking ζ and the temperature Θ. When assuming constant and homogeneous temperatures $\Theta = \Theta_{h}$ within the sample the torque response $\widehat{M}(t)$ can be approximated for small phase angles $\delta(t)$ by

$$\widehat{M}(t) = \frac{\mu^{e}(t) I_{T}}{h}\hat{\varphi} \tag{90}$$

$$= (p_1 + p_2\zeta(t)) f_1(\Theta_h)\frac{I_{T}}{h}\hat{\varphi} \tag{91}$$

$$= \widehat{M}_{\min} + (\widehat{M}_{\max} - \widehat{M}_{\min})\zeta(t). \tag{92}$$

The values of $\widehat{M}_{\min}$ and $\widehat{M}_{\max}$ can be directly determined for each test result. Several measurements of $\widehat{M}(t)$ performed at different temperatures Θ_h allow the determination of the curing parameters k_1, k_2, k_3, k_4, α and β which are used in Eqs. (22) and (23) of the vulcanization model. Fig. 11 shows the results of this analytical approach in conjunction with the identified parameters compared to the measured vulkameter test data. The identification has been done by using heating temperatures in the range of $\Theta_h = 140\ ^{\circ}\mathrm{C}, \ldots, 220\ ^{\circ}\mathrm{C}$. Since the transient thermal conduction process causes temperature inhomogeneities at the beginning of the measurement which are neglected in this simplified analytic approach, there are some deviations visible at the beginning of the 140 °C-curve.

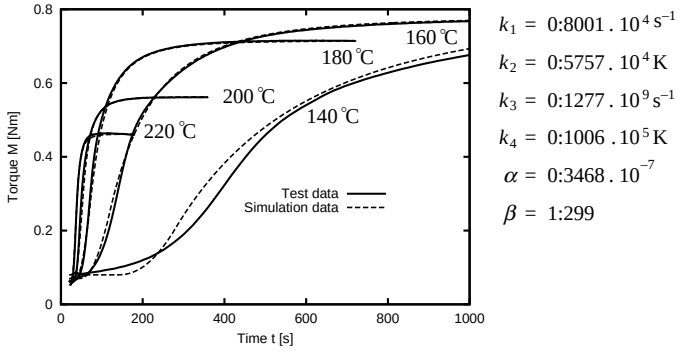

Fig. 11. Result of identification of curing parameters.

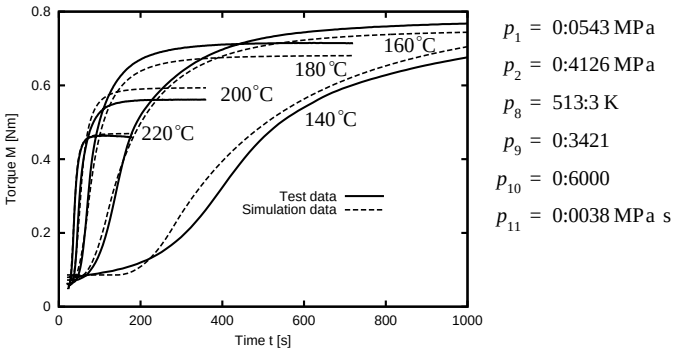

Fig. 12. Identification of the visco-elastic constitutive parameters.

4.2.2. Visco-elastic parameters

Besides the determination of the curing parameters, the vulkameter test also allows the identification of visco-elastic material properties. The simplified rheological model described by Eqs. (87) and (89) can be compared to the measured torque response of the vulkameter. Now the in-phase part $\widehat{M}^{*}(t)$ and the phase angle $\delta(t)$ of the experimental data are used to determine the parameters p_1, p_2, p_8, p_9, p_{10} and p_{11}. Within this identification the previously determined kinetics of the curing process are already used. Fig. 12 shows the results of this approach in comparison to the measured vulkameter data.

4.3. Uniaxial compression tests

The vulkameter test is suitable to characterize short-term visco-elastic effects with a characteristic time constant τ^{ve_1} being in the same order as the period $T = \frac{2\pi}{\omega}$ of a torsion cycle. If viscous effects with a much higher viscosity are of interest, other experimental setups are needed. For this purpose a uniaxial compression test as shown in Fig. 13 is used. Cylindrical rubber samples are cured until a defined state of cross-linking is reached. The compression is applied according to a displacement function $u(t)$ as defined in Fig. 14 and the force response $F(t)$ is measured. Here it should be noted that it is not always possible to apply a tension to such a sample, since uncured samples usually cannot be fixed properly. After a certain time during which the force has continuously decreased, the sample is unloaded and stored for a sufficiently long time. Then the residual deformation u_{in} is measured and used to determine the inelastic deformation ϵ^{vp}.

Because of the fixed boundary conditions at the upper and lower side of the specimen the deformation field $\boldsymbol{\epsilon}(\boldsymbol{x},t)$ and the stress field $\boldsymbol{\sigma}(\boldsymbol{x},t)$ are not homogeneous. In order to achieve an easy-to-handle, uniaxial

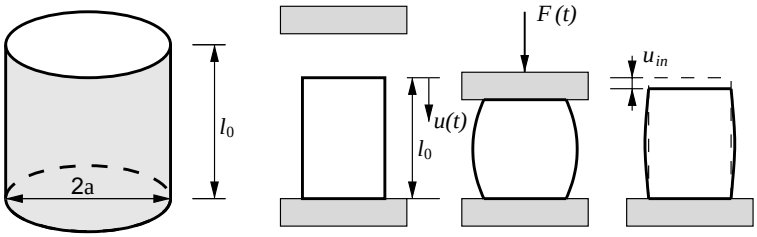

Fig. 13. Uniaxial compression test.

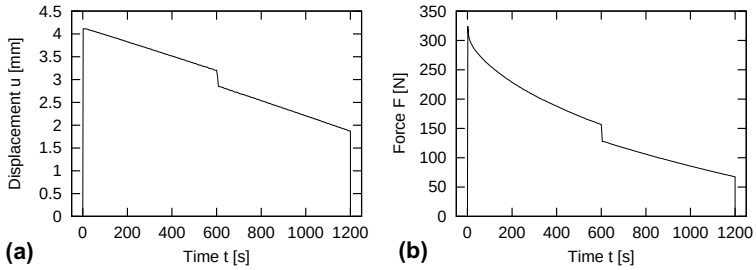

Fig. 14. (a) Applied displacement $u(t)$ and (b) measured force $F(t)$ of compression test.

approach for the parameter identification, the stresses and strains are needed to be averaged. The averaged uniaxial strains $\bar{\epsilon}(t)$ are defined by

$$\bar{\epsilon}(t) = -u(t)/l_0 \tag{93}$$

and the averaged uniaxial stress $\bar{\sigma}(t)$ is approximated by the approach

$$\bar{\sigma}(t) = \bar{C}(\bar{\epsilon})\frac{F(t)}{\pi a^2}, \tag{94}$$

where the function

$$\bar{C}(\bar{\epsilon}) = c_1\ \bar{\epsilon}^{c_2} \tag{95}$$

covers all effects resulting from the inhomogeneities and the nonlinear kinematics. The elastic material properties are assumed to be linear within the investigated strain range. The quality of this correction approach is shown in Fig. 15, where the corrected analytical force response of a linear-elastic material is compared to a three-dimensional finite-element simulation. From this comparison the parameters in the correction function are determined by $c_1 = 3.1$ and $c_2 = 1.3$.

With this approach the stress response of the uniaxial compression test can be described by the following equations that cover all the effects of the introduced material model

$$\bar{\epsilon} = \bar{\epsilon}^{\mathrm{e}} + \bar{\epsilon}^{\mathrm{ve}_1} + \bar{\epsilon}^{\mathrm{ve}_2} + \bar{\epsilon}^{\mathrm{vp}}, \tag{96}$$

$$\bar{\sigma} = E^{\mathrm{e}}\bar{\epsilon}^{\mathrm{e}}, \tag{97}$$

$$\dot{\bar{\epsilon}}^{\mathrm{ve}_1} = B_1\bar{\epsilon}^{\mathrm{e}} - B_2\bar{\epsilon}^{\mathrm{ve}_1}, \tag{98}$$

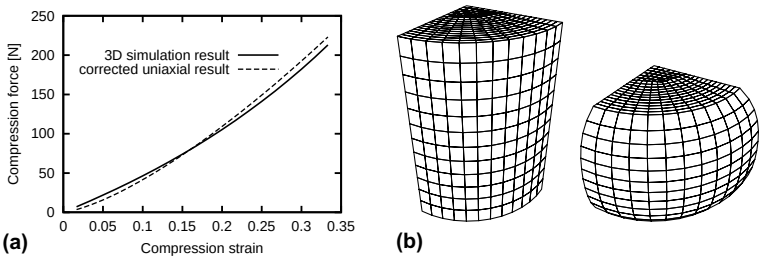

Fig. 15. (a) Comparison of 3D Finite Element simulation and correction for uniaxial approach and (b) FE mesh of sample under compression.

$$\dot{\bar{\epsilon}}^{\mathrm{ve}_2} = B_3\bar{\epsilon}^{\mathrm{e}} - B_4\bar{\epsilon}^{\mathrm{ve}_2}, \tag{99}$$

$$\dot{\bar{\epsilon}}^{\mathrm{vp}} = \frac{1}{\eta^{\mathrm{vp}}}\langle\bar{\sigma} - \sigma_{\mathrm{f}}\rangle, \tag{100}$$

with

$$E^{\mathrm{e}} = 2(1+\nu)\mu^{\mathrm{e}} \approx 3\mu^{\mathrm{e}}, \tag{101}$$

$$\sigma_{\mathrm{f}} = \sqrt{3}k_{\mathrm{f}}. \tag{102}$$

These equations can easily be integrated by an explicit time integration scheme. The stress response $\bar{\sigma}(t)$ then can be compared to the measured forces $F(t)$ by use of the correction described above. Additionally, the residual (plastic) deformation at the end of the experiment is used for the parameter identification. This allows to determine the parameters p_3, p_4, p_5, p_6, p_7 and p_{12} of the material model. All other parameters have already been determined from the previously described experiments and can be used in Eqs. (97)–(102).

Fig. 16(a)–(c) shows the results of this approach and the parameter identification in comparison to the measured uniaxial compression data. One can observe that the predicted data do match the experimental curves very well.

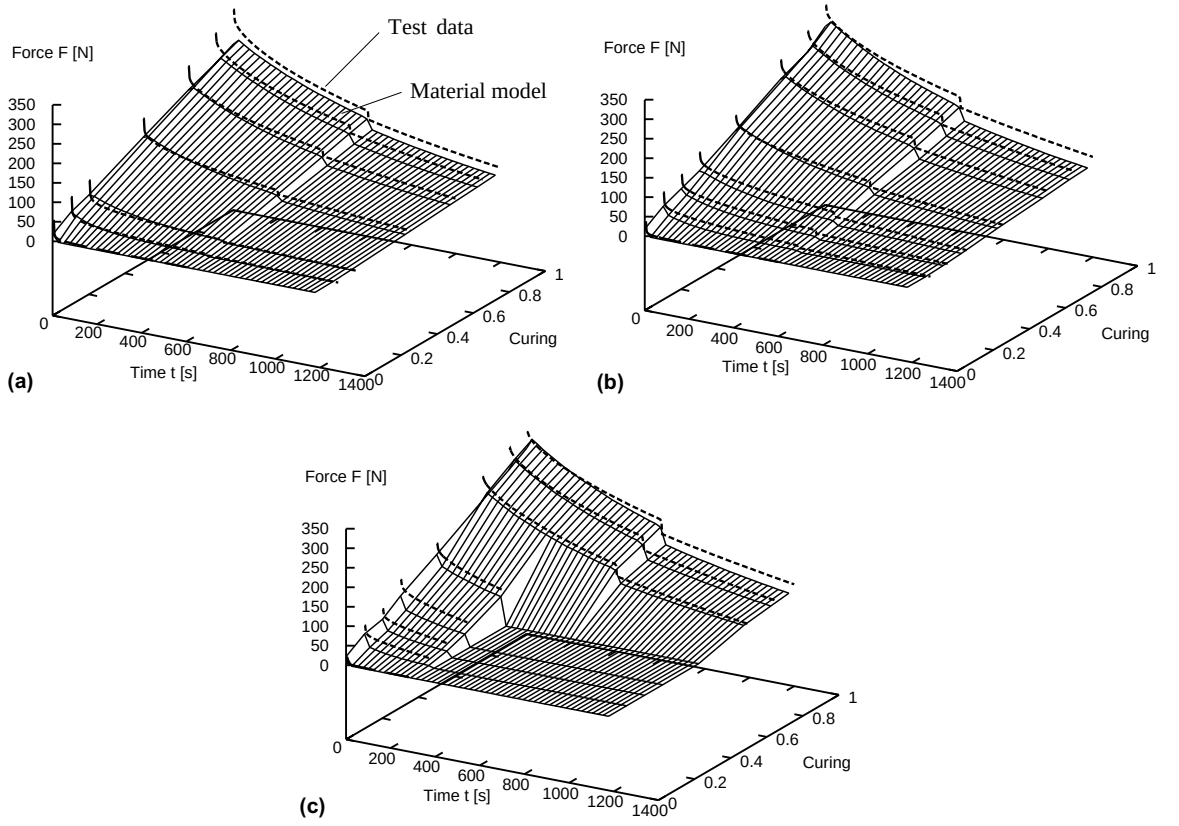

Fig. 16. Experimental data and results of material model at: (a) $\Theta = 50$ °C; (b) $\Theta = 80$ °C and (c) $\Theta = 120$ °C.

5. Conclusion

In this paper we have developed a constitutive model for the coupled chemo-thermo-mechanical process of vulcanization. This material model can be applied to predict the vulcanization time and the associated state as well as the mechanical response (deformations and residual stresses) within a rubber part. For these the governing field equations and the evolution equations which are highly nonlinear have to be solved using a numerical method. In this connection the authors have developed a finite element scheme which is reported in another paper.

Future work in this area has to include large strain effects to make the developed constitutive equation applicable to a broader range of industrial problems in the area of forming rubber parts.

References

Adolf, D.B., et al., 1998. Stresses during thermoset cure. J. Mater. Res. 13 (3), 530–550.
Aklonis, J.J., MacKnight, W.J., 1983. Introduction to Polymer Viscoelasticity. Wiley, New York.
Atkins, P.W., 1982. Physical Chemistry, second ed. Oxford University Press.
Coleman, B.D., 1964. Thermodynamics of materials with memory. Arch. Ration. Mech. Anal. 17, 1–46.
Coleman, B.D., Gurtin, M.E., 1967. Thermodynamics with internal state variables. J. Chem. Phys. 47 (2), 597–613.
Davis, L., 1991. Handbook of Genetic Algorithms. Van Nostrand Reinhold, New York.
Ferry, J.D., 1980. Viscoelastic Properties of Polymers. Wiley, New York.
Haupt, P., Olt, V., 1989. Temperatureinfluesse bei der Beschreibung der Kautschukvernetzung durch innere Variable. Zeitschrift fuer angewandte Mathematik und Mechanik 69, 474–476.
Kaliske, M., Rothert, H., 1997. Formulation and implementation of three-dimensional viscoelasticity at small and finite strains. Computat. Mech. 19 (17), 228–239.
Kaliske, M., Rothert, H., 1998. Constitutive approach to rate-independent properties of filled elastomers. Int. J. Solids Struct. 35 (17), 2057–2071.
Laidler, K.J., 1963. Reaction Kinetics. Pergamon Press, Oxford, London, New York, Paris.
Mahnken, R., 1993. The identification of parameters for visco-plastic models via finite-element methods and gradient methods. Model. Simul. Mater. Sci. Eng. 2, 597–616.
Mark, J.E., 1994. Science and Technology of Rubber. Academic Press, San Diego.
Mooney, M., 1940. A theory of large elastic deformation. Journal of Applied Physics 11, 582–592.
Ogden, R.W., 1972. Large deformation isotropic elasticity: on the correlation of theory and experiment for incompressible rubberlike solids. Proceedings of the Royal Society of London Series A 326, 565–584.
Ogden, R.W., 1984. Non-linear Elastic Deformations. E. Horwood and J. Wiley, Chichester.
Schmidt, L.D., 1998. The Engineering of Chemical Reactions. Oxford University Press, New York, Oxford.
Simo, J.C., Hughes, T.J.R., 1998. Computational Inelasticity. Springer Verlag, New York.
Treloar, L.R.G., 1975. The Physics of Rubber Elasticity. Clarendon Press, Oxford.
Yeo, M.F., Agyei, E.O., 1998. Optimising engineering problems using genetic algorithms. Engineering Computations 15 (2), 268–280.